

Predicting particle deposition on HVAC heat exchangers

Jeffrey A. Siegel^{a,*}, William W Nazaroff^b

^a Architectural Engineering Program, Department of Civil Engineering, University of Texas, Austin, TX, 78712-1076, USA

^b Department of Civil and Environmental Engineering, University of California, Berkeley, CA, 94720-1710, USA

Received 3 April 2003; received in revised form 30 July 2003; accepted 8 September 2003

Abstract

Particles in indoor environments may deposit on the surfaces of heat exchangers that are used in heating, ventilation and air conditioning (HVAC) systems. Such deposits can lead to performance degradation and indoor air quality problems. We present a model of fin-and-tube heat-exchanger fouling that deterministically simulates particle impaction, gravitational settling, and Brownian diffusion and uses a Monte Carlo simulation to account for impaction due to air turbulence. The model predicts that <2% of submicron particles will deposit on heat exchangers with air flows and fin spacings that are typical of HVAC systems. For supermicron particles, deposition increases with particle size. The dominant deposition mechanism for 1–10 μm particles is impaction on fin edges. Gravitational settling, impaction, and air turbulence contribute to deposition for particles larger than 10 μm . Gravitational settling is the dominant deposition mechanism for lower air velocities, and impaction on refrigerant tubes is dominant for higher velocities. We measured deposition fractions for 1–16 μm particles at three characteristic air velocities. On average, the measured results show more deposition than the model predicts for an air speed of 1.5 m s^{-1} . The amount that the model underpredicts the measured data increases at higher velocities and especially for larger particles, although the model shows good qualitative agreement with the measured deposition fractions. Discontinuities in the heat-exchanger fins are hypothesized to be responsible for the increase in measured deposition. The model and experiments reported here are for isothermal conditions and do not address the potentially important effects of heat transfer and water phase change on deposition.

© 2003 Elsevier Ltd. All rights reserved.

Keywords: Particle deposition; Heat-exchanger fouling; Ventilation systems; Deposition mechanisms; Energy efficiency

1. Introduction

Heat exchangers are used widely in industrial processes, electricity generation, and heating, ventilation and air conditioning (HVAC) systems. Invariably, these heat-exchangers foul. Fouled heat exchangers have diminished heat transfer performance, increased pressure drop, and can cause contamination of working fluids. The serious financial and performance consequences of these problems have raised the profile of heat-exchanger fouling as an important area of study.

Several conferences (Somerscales and Knudsen, 1981; Melo et al., 1988) and research initiatives (Tabourek et al., 1972; Bott, 2001) have focused on the fouling problem.

Despite these efforts, engineers have largely overlooked fouling of HVAC heat exchangers. Fouled heating and cooling systems can significantly increase energy use and decrease heating and cooling performance; fouling also can cause indoor air quality degradation. Particulate fouling of indoor fin-and-tube heat exchangers, particularly air conditioner evaporators, necessitates study because space cooling in buildings is an important contributor to overall energy use and peak electricity demand (Proctor, 1998). Furthermore, microorganisms can colonize persistently moist

*Corresponding author. Tel.: +1-512-471-2410; fax: +1-512-471-3191.

E-mail address: jasiegel@mail.utexas.edu (J.A. Siegel).

surfaces of cooling coils, causing indoor bioaerosol problems (Hugenholz and Fuerst, 1992; Morey, 1988).

Although technical reports, trade journals, and manufacturers' literature discuss cleaning and maintaining HVAC heat exchangers, little has been written about the factors that control HVAC heat-exchanger fouling by deposition of particulate matter. Researchers have modeled particulate fouling for heat exchangers used in industrial processes. They have made significant strides in the modeling fouling mechanisms in dairy processing (Petermeier et al., 2002), nuclear reactor cooling systems (Rampall et al., 1997), crude oil distillation (Mukherjee, 1996), and other process and industrial heat exchangers. This body of work is important and has improved many of the processes that use heat exchangers, but several limitations prevent its application to the specific problem of HVAC heat-exchanger fouling. The first limitation is geometric. The fin-and-tube heat exchangers that are typical of HVAC systems are not widely used in industrial processes, and the existing models are not typically adaptable to different geometries. The second limitation is one of medium. Many of the problems in the literature involve fouling of the liquid side of a heat exchanger. Although the physics do not change as the medium changes, the limiting mechanisms for fouling of liquid systems are often crystallization or precipitation reactions. These reactions are less important in HVAC heat-exchanger fouling and other low temperature particulate and gas fouling problems. The third limitation has to do with the purpose of process heat-exchanger fouling work. In many studies, it has been less important to understand the mechanisms than to find solutions. This practical orientation limits the applicability of the work beyond the direct circumstances studied.

The objective of this paper is to develop and test a model of particle deposition in typical HVAC heat exchangers. The development of this model represents an important step toward the evaluation of energy and indoor air quality effects of heat-exchanger fouling. The model is simple and general enough that it can be applied to a wide range of heat exchangers. The model uses three major inputs (air velocity, particle size, and fin spacing) and several minor inputs to determine the likelihood that a particle will deposit in a heat exchanger. The paper also summarizes laboratory experiments that test model performance. The work presented here is restricted to isothermal conditions.

The major output of the model is the deposition fraction, η , defined as the likelihood that a particle of a given size will deposit on a heat exchanger. The mass deposition rate of particles of a given diameter is the product of the deposition fraction, the flow rate of air through the heat exchanger, and the concentration of particles in the air upstream of the heat exchanger. Owing to the importance of particle diameter on

deposition processes, the deposition fraction is a function of particle size. Air velocity also affects the deposition fraction by altering the inertial impaction of particles as well as the residence time of particles in the heat exchanger. Fin spacing, a geometric parameter that is related to heat-exchanger thermal efficiency and pressure drop, influences the deposition fraction by changing the distance that a particle must travel to contact a surface.

In this paper, we seek estimates of the deposition fraction and the factors that influence it. The primary focus is a mathematical model of deposition in a fin-and-tube heat exchanger that accounts for inertial impaction, gravitation settling, air turbulence and Brownian diffusion. We also test the model with data from experiments for a typical HVAC heat-exchanger geometry and for representative airflows in HVAC systems.

2. System characterization and methods

2.1. System description

2.1.1. Heat exchangers

For the purposes of modeling, the fin-and-tube heat-exchanger geometry is represented as a series of straight vertical channels created by the fins with cylindrical refrigerant tubes that run horizontally, perpendicular to the fins. The fins are often corrugated to increase the heat transfer area. A schematic of typical fin-and-tube heat-exchanger geometry appears in Fig. 1.

Several parameters describe heat-exchanger coil geometry. Fin pitch, the metric usually used to describe fin spacing, ranges from 2.4 fins cm^{-1} for low efficiency

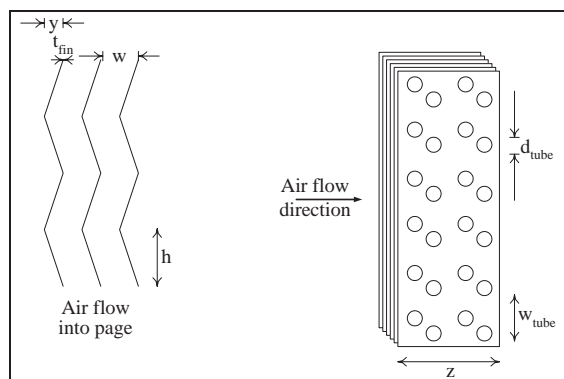


Fig. 1. Front view of leading edge of fins (left) and side view of heat exchanger and refrigerant tubes (right). Here w is the center-to-center fin spacing, h is the average height of fin corrugations, t_{fin} is the fin thickness, y is the peak to trough width of fin corrugations, d_{tube} is the tube diameter, w_{tube} is the tube spacing, z is the heat-exchanger depth. The heat-exchanger pictured has four tube rows, $n_{\text{row}} = 4$, and two sets of offset tubes, $n_{\text{offset}} = 2$.

heating coils (where heat transfer efficiency is not as important as capital cost) to 7.1 fins cm⁻¹ for very high efficiency cooling coils. A typical fin pitch for a Freon refrigerant heating or cooling coil is 4.7 fins cm⁻¹. In addition to the fins, refrigerant tubes are an important part of the heat exchanger. The tube diameter is usually selected based on the refrigerant and capacity requirements for the heat exchanger, and ranges from 1 cm for Freon refrigerant systems to 5 cm for chilled water and steam coils. The number of vertical rows, n_{rows} , of tubes affects capacity, and tube rows are often offset to improve heat transfer and to facilitate manufacture and refrigerant flow. Geometric parameters for the heat exchanger analyzed in this paper are typical of those in residential and small commercial buildings (see Table 1).

2.1.2. Characteristics of airflow in heat exchangers

The air velocity through a heat-exchanger influences particle inertia, residence time, and air turbulence. The bulk velocity is the ratio of volumetric air flowrate through the section of duct where the heat exchanger is located to the cross-sectional area of the duct. Design air velocities in HVAC systems range from 1 ms⁻¹ for residential central air-conditioning and commercial reheat coils to 4 ms⁻¹ for plenums in large commercial systems. Three Reynolds numbers are relevant for characterizing airflow in heat exchangers: Re_{duct} is based on the characteristic cross-flow dimension of the duct,

Re_{fin} is based on the spacing between the fins, and Re_{tube} is based on the diameter of the refrigerant tubes. Characteristic values for these parameters in HVAC heat exchangers appear in Table 2.

2.1.3. Characteristics of airborne fouling agents

Particulate fouling depends critically on particle diameter. Previous work on heat-exchanger fouling has emphasized supermicron particles since these particles are sufficiently large to cause a significant fouling layer when they deposit (Bott and Bemrose, 1983; Muyschondt et al., 1998). However, submicron particles exist at much higher concentrations in typical indoor environments, so this study will consider particles as small as 0.01 μm in diameter. Particles in the size range 0.01–1 μm exist in indoor environments as the result of combustion (including tobacco smoke), penetration from outdoor sources, and gas-to-particle conversion processes. Particles in the range 1–10 μm include some soil grains, certain bioaerosols, and particles from cooking and other household activities. Very large particles, with diameters from 10 to 100 μm, are found in indoor dusts. It is important to note that even smaller particles than considered here (i.e. those with a characteristic dimension of 10 nm or smaller) do exist in indoor environments. However, these very small particles are present at very low mass concentrations and so are unlikely to contribute significantly to pressure drop or thermal resistance.

2.2. Analysis of particle deposition in heat exchangers

We consider deposition of particles by impaction on fin edges and refrigerant tubes, gravitational settling on fin corrugations, impaction on fin walls by turbulent motion, and deposition by Brownian motion. These deposition mechanisms are described below. Particle transport to heat-exchanger surfaces is calculated deterministically for each deposition mechanism except for turbulent impaction. Air turbulence is simulated with a Monte Carlo scheme. For all deposition mechanisms, particles are assumed to adhere when they contact a surface. The assumption of perfect sticking is

Table 1
Parameters for modeled heat exchanger

Parameter		Dimension
t_{fin}	Fin thickness	0.114 mm
d_{tube}	Tube outer diameter	9.53 mm
w	Fin-to-fin spacing	1.4, 2.1, 4.2 mm
w_{tube}	Center-to-center tube spacing	25.4 mm
z	Fin depth	44 mm
h	Fin corrugation average height	1.5 mm
y	Fin corrugation width	1.0 mm
n_{row}	Number of tube rows	4
n_{offset}	Number of offset rows	2

Table 2
Reynolds numbers in HVAC heat exchangers

Parameter	Formula ^a	Typical range in HVAC systems
Reynolds number based on duct dimension	$Re_{\text{duct}} = \frac{d_{\text{duct}} U}{\nu}$	10 ⁴ –10 ⁵
Reynolds number in fin channels	$Re_{\text{fin}} = \frac{(w - t_{\text{fin}}) U_{\text{fin}}}{\nu}$	10 ² –10 ³
Reynolds number based on tube diameter	$Re_{\text{tube}} = \frac{d_{\text{tube}} U_{\text{fin}}}{\nu}$	10 ³ –10 ⁴

^a d_{duct} is the duct diameter, U the bulk air velocity in the duct, ν the kinematic viscosity of air, w the center-center fin spacing, t_{fin} the fin thickness, U_{fin} the bulk air velocity in the fin channels, and d_{tube} the refrigerant tube outer diameter.

likely to apply early in the fouling process as most heat-exchanger surfaces are coated with oils from the manufacturing process. Furthermore, our verification experiments were conducted with liquid particles, which adhere to surfaces upon contact. Particle bounce and resuspension of previously deposited material were not directly addressed in this study.

2.2.1. Impaction on fins edges

Field examination of fouled heat exchangers suggests that impaction on the leading edge of the fins is an important deposition mechanism. For this analysis, we assume that the fin edge is a blunt body and use Hinds' (1999) analysis for rectangular slit cascade impactors with a modification to account for the fraction of face area of the heat exchanger that is occupied by fin edges. The analysis assumes that the air approaching the fin edge makes a 90° bend. The penetration fraction accounting only for losses because of impaction on fin edges, P_{fin} , is estimated as follows:

$$P_{\text{fin}} = 1 - \left(Stk_{\text{fin}} \frac{\pi}{2} \right) \frac{t_{\text{fin}}}{w} cf, \quad (1)$$

where Stk_{fin} is the particle Stokes number based on the duct air velocity and the fin thickness, corrected for particles having particle Reynolds numbers > 0.1 (Israel and Rosner, 1983), t_{fin} is the fin thickness, w is the center-to-center fin spacing, and cf is the corrugation factor. The corrugation factor takes into account the fact that a corrugated fin is longer than a straight fin and thus has more leading edge area for particle impaction. The corrugation factor is defined as $(y^2 + h^2)^{0.5} h^{-1}$ where h is the average height of the fin corrugations and y is the peak-to-trough corrugation width (see Fig. 1). The term in parentheses in Eq. (1) is limited to a maximum value of one to limit deposition only to the fraction of particles that are directly in front of each fin.

Hinds (1999) estimates a 10% uncertainty bound on deposition $(1 - P_{\text{fin}})$ for cascade impactors. In the most extreme case, with dense fin spacing, the factor $t_{\text{fin}} \times cf \times w^{-1}$ is 10%. Thus the absolute estimated error in P_{fin} is $\sim 1\%$ or less. The true uncertainty is probably larger, since Eq. (1) was developed for deposition from laminar flow in a cascade impactor rather than on the leading edge of heat-exchanger fins. The fin edges are much thinner than cascade impactor plates and thus would cause a lesser disturbance of fluid streamlines. We expect that the thinner fin edges would cause Eq. (1) to underpredict the penetration associated with fin edge-impaction. Furthermore, the air flow near heat exchanger fins often has turbulent characteristics, which we would expect to increase deposition on fin edges. To further explore uncertainty, an alternative estimate of the penetration fraction for this mechanism was calculated assuming that the fin edges were vertical half-cylinders with diameter equal to the fin thickness. A

modification of the work of Wang (1986) for deposition of particles from turbulent flow onto circular cylinders was used:

$$P_{\text{fin,round}} = 1 - \frac{2}{\pi} \arctan \left(0.8 \left(Stk_{\text{fin}} - \frac{1}{8} \right)^{0.8} \right) \frac{t_{\text{fin}}}{w} cf. \quad (2)$$

The penetration associated with deposition on fin edges was estimated from Eq. (1) with uncertainty bounds determined by selecting the highest and lowest values from Eq. (1), including the 10% uncertainty, and Eq. (2).

2.2.2. Impaction on refrigerant tubes

Particles may also impact on the refrigerant tubes that are normal to both the airflow direction and the fins. The penetration fraction associated with deposition on the refrigerant tubes was estimated from Wang (1986) for the relevant Re_{tube} range, modified to account for multiple rows of offset tubes:

$$P_{\text{tube}} = \left(1 - \frac{2}{\pi} \arctan \left(0.8 \left(Stk_{\text{tube}} - \frac{1}{8} \right)^{0.8} \right) \times \frac{d_{\text{tube}}}{w_{\text{tube}}} n_{\text{offset}} \right)^{n_{\text{row}}/n_{\text{offset}}} \quad (3)$$

where Stk_{tube} is the particle Stokes number based on the bulk air velocity in the heat exchanger and d_{tube} , the tube diameter; w_{tube} is the center-to-center vertical tube spacing; n_{offset} is the number of offset rows; and n_{row} is the number of tube rows (see Fig. 1).

There are several important assumptions that must be made to allow the use of Eq. (3). The first is that each tube can be considered to be independent of the other tubes in the system. The simulations and experimental work of Ilias and Douglas (1989) suggest that this is a good assumption for tubes in a vertical plane with tube spacings typical of those in HVAC heat exchangers. However, the wake of upstream tubes can alter deposition for downstream rows of tubes. Braun and Kudriavtsev (1995) conducted numerical flow simulations for flow past a tube network with $d_{\text{tube}} = w_{\text{tube}} = z_{\text{tube}}$, where z_{tube} is the tube spacing in the direction of flow. The flow fields in their work suggest that the wake effect can lead to greatly increased turbulence on downstream tubes at Re_{tube} typical of HVAC heat exchangers. This greater turbulence would in turn lead to increased particle deposition, although the magnitude of this effect is unclear. The narrow fin channels tend to decrease air turbulence, and geometric features that are designed to restart the boundary layers and promote turbulence tend to increase air turbulence. The effect of tube wake was not included in this analysis because of lack of data on turbulence characteristics in a representative geometry.

The second assumption is that the particles are uniformly mixed as they approach each tube. Although the tube wakes promote mixing, the short characteristic time that it takes particles to travel between the sets of tubes [O(10ms)] means that the assumed uniform particle concentration, particularly, at high enough Stk_{tube} to cause significant deposition ($Stk_{\text{tube}} \gtrsim 1$), is unlikely to be correct for downstream tube rows. Bouris and Bergeles (1996) document this shielding effect for a very high flow system ($Re_{\text{tube}} = 1.3 \times 10^4$) with very large particles (45–700 μm). Their experimental work in a combustion boiler heat exchanger suggests that about 80% less deposition occurs on the second row of aligned tubes. Their work is not directly applicable (because of the high Reynolds numbers and large particle sizes), but it does suggest that the shielding effect can be significant. This would then lead to Eq. (3) overestimating deposition. To establish the upper bound on P_{tube} resulting from the shielding effects, calculations were also done assuming complete shielding (i.e. only considering deposition on the first two vertical row of tubes in Fig. 1). In all cases, impaction on tubes was only considered for particles directly in front of each refrigerant tube.

2.2.3. Gravitational settling

To increase heat transfer, manufacturers often corrugate fins. Large particles can deposit by gravitational settling on the corrugation surfaces that possess a horizontal component. The penetration fraction accounting for losses only from gravitational settling, P_G , is estimated as follows (Fuchs, 1964):

$$P_G = 1 - \left(\frac{V_s Z}{hU} \right) \frac{y}{w - t_{\text{fin}}}, \quad (4)$$

where V_s is the particle settling velocity, z the heat exchanger depth in the direction of bulk air flow, and U the bulk air velocity in the heat exchanger. The ratio in parentheses is limited to a maximum value of one.

The largest uncertainty for deposition associated with gravitational settling is that the vertical channel geometry considered by Fuchs (1964) is significantly different than the sloped channel geometry that occurs in the fin corrugations. Furthermore Fuchs' analysis was limited to laminar flow rather than the transition flow common in heat exchangers. Several researchers have considered gravitational settling in horizontal tubes (e.g. Pich, 1972) and inclined tubes (e.g. Lipatov et al., 1988; Anand et al., 1992), but these geometries are even less applicable because of their circular cross section or the fact that they slope in the direction of flow, rather than across the channel as occurs in a fin corrugation. To assess the variation in deposition by gravitational settling, an upper bound on the penetration fraction associated with this mechanism was made by doubling the average height of the fin corrugation. Similarly, a

lower bound was estimated by halving the average height of the fin corrugation.

2.2.4. Air turbulence

Air turbulence in the duct leading up to a heat exchanger can also induce deposition on heat-exchanger surfaces. The fluctuating components of velocity can impart an angled trajectory to particles as they enter the heat-exchanger channels. If the particle has a sufficiently large relaxation time and a sufficient deviation in velocity direction from the bulk flow, it will impact on a fin and not penetrate the coil.

We estimate the penetration associated with losses owing to turbulent deposition as follows:

$$P_T = \text{Prob} \left(\frac{\tau_{\text{imp}}}{\tau_p} > 1 \right), \quad (5)$$

where τ_{imp} is the characteristic time for a particle to impact on the wall and τ_p is the particle relaxation time. The impaction time scale, τ_{imp} is calculated from geometry and trigonometry as follows:

$$\tau_{\text{imp}} = \frac{w_T}{v'_p}, \quad (6)$$

where w_T is the distance from the nearest fin when the particle enters the channel and v'_p is the particle turbulence fluctuating velocity component perpendicular to the fin channel at a given particle entering location.

Unlike the deterministic calculations used to assess the other deposition mechanisms, a Monte Carlo simulation was used to estimate P_T . For a given particle size, 10^7 simulations were completed to minimize any numerical uncertainty. In the analysis, particles were assumed to enter the channel uniformly distributed between the fins, by selecting w_T from a uniform distribution with maximum value of $(w - t_{\text{fin}})/2$. The fluctuating components of the air velocity were assumed to be independent Gaussian distributions whose shape, as a (weak) function of bulk velocity in the duct, was obtained from direct numerical simulation (DNS) data presented by Moser et al. (1999). Although we are considering impaction by air turbulence as a two-dimensional phenomenon (because the vertical component of fluctuating velocity will not lead to significant increased deposition), the Moser et al. (1999) simulations consider all three dimensions.

The assumption of a Gaussian air turbulence distribution is common for many problems (Hinze, 1959) and has been used for the specific problem of HVAC heat-exchanger fouling (Muyschondt et al., 1998). It is important to note that, because no turbulence measurements have been reported for flow through a comparable heat exchanger, the actual spatial distribution of the turbulent fluctuations is unknown. Also, the geometry of Moser et al. (1999) simulations are for a channel,

rather than the duct flow upstream of the coil; consequently, our use of the data represents an extrapolation whose accuracy is unknown.

The analysis presented in Eqs. (5) and (6) also assumes that the turbulence does not persist from the bulk flow into the fin channels. This assumption is justified by the fact that the largest turbulent eddies are the most persistent and contain the most turbulent energy (Hinze, 1959). These large eddies from the bulk duct flow are broken up or constrained by the narrow dimension of the fin channels. In an idealized case, the flow would relaminarize. However, real heat exchangers contain macroscale roughness elements and fin discontinuities, which are designed to promote turbulence and restart the boundary layer to increase heat transfer. The exact nature of the turbulent flow in the heat exchanger is unknown, but it is likely that turbulence would enhance deposition in the channels.

The role of turbulence in inducing deposition onto the refrigerant tubes was also considered. The lower bound on P_{tube} was accounted for by including deposition by turbophoresis, the motion of particles down a turbulence intensity gradient. Since this was intended to be a bounding estimate, we assumed that the duct turbulence parameters persisted all the way through the fin channels in the heat exchanger. The magnitude of deposition owing to turbophoresis was calculated following the work of Caporaloni et al. (1975). The velocity component of the particle towards the wall due to turbophoresis, v_{TB} , was calculated as follows:

$$v_{\text{TB}} = -\tau_p \left(\frac{d(v_p'^2)}{dx} \right), \quad (7)$$

where the derivative term is the slope of the squared fluctuating particle velocity component in the direction normal to the fin. The turbulence parameters were taken from the DNS work of Moser et al. (1999). The penetration fraction as a result of deposition by turbophoresis was calculated as follows:

$$P_{\text{TB}} = 1 - \left(\frac{2v_{\text{TB}}z}{(w - t_{\text{fin}})(U + u_p')} \right), \quad (8)$$

where u_p' is the fluctuating component of the velocity in the direction of the bulk air flow.

2.2.5. Brownian diffusion

Very small particles are most likely to deposit onto heat-exchanger surfaces by means of Brownian diffusion. The penetration fraction accounting for deposition only by Brownian diffusion was calculated assuming laminar flow in the heat exchanger core, following the work of DeMarcus and Thomas (1952) for channel flow:

$$P_{\text{D}} = 0.915e^{(-1.885\xi)} + 0.0592e^{(-22.3\xi)} + 0.0259e^{(-152\xi)}, \quad (9)$$

where $\xi = 4Dz/[(w - t_{\text{fin}})^2U]$ and D is the particle diffusion coefficient equal to $kTC_c(3\mu d_p\pi)^{-1}$ where k is the Boltzmann constant, T is the air temperature, and μ is the dynamic viscosity of the air.

Brownian diffusion was included in the model because it is the only potentially significant deposition mechanism for submicron particles in this system (at least for the isothermal case that we are considering here). Nevertheless, due to the relatively short residence time in the system at typical velocities, particles of interest do not deposit significantly by Brownian diffusion. Hence, no uncertainty estimate was included for this deposition mechanism.

2.2.6. Combining deposition mechanisms

The deposition mechanisms were combined assuming that they act independently so that the overall deposition fraction, η , was estimated by Eq. (10). The assumption of independence is well justified for mechanisms that affect widely different particle sizes, such as Brownian diffusion and gravitational settling (Chen and Yu, 1993). The assumption has been applied to estimate deposition by combined mechanisms in heat exchangers (Bott, 1988; Epstein, 1988) and in other systems, such as fibrous filtration (Hinds, 1999).

$$\eta = 1 - P_{\text{fin}}P_{\text{tube}}P_{\text{G}}P_{\text{T}}P_{\text{D}}. \quad (10)$$

Each term in Eq. (10) is limited to be between one and zero.

The overall uncertainty in the calculation of η was determined by estimating an upper and lower bound for each of the penetration factors in Eq. (10), except Brownian diffusion, because of its minimal importance to overall deposition. The lower bound on η was calculated by substituting the maximum values for each of the penetration factors in Eq. (10) and the upper bound was calculated with the minimum values.

2.3. Experimental verification

Experiments were conducted to test the modeling predictions using the apparatus depicted in Fig. 2. Monodisperse oil particles, tagged with fluorescein, were generated with a vibrating orifice aerosol generator (TSI model 3450) and then charge neutralized (TSI model 3054). Air from the particle generator was diluted with HEPA-filtered air and sent into 24 m of straight 15 cm × 15 cm square duct. Several honeycomb flow straighteners were used to promote fully developed turbulent flow with a uniform concentration of test particles. The particle-laden air then passed through an experimental 4.7 fin cm⁻¹ heat exchanger (other geometric parameters are described in Table 2) that entirely filled the duct. The test heat exchanger is typical of those found in residential and light commercial buildings.

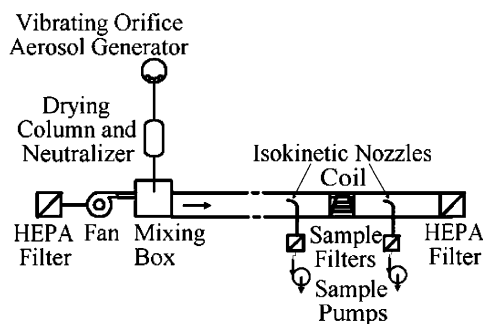


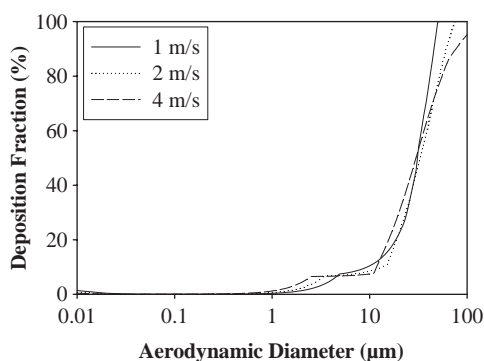
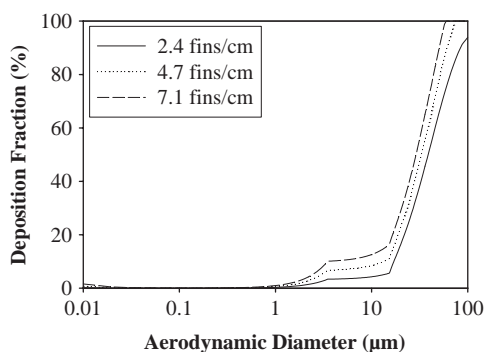
Fig. 2. Experimental apparatus.

The particle size was determined with an aerodynamic particle sizer (TSI model 3320). Airborne particle concentrations were measured upstream and downstream of the heat exchanger by isokinetically sampling the air onto filters, which were later analyzed by fluorometric techniques (Turner Designs model TD-700 fluorometer). The coil and the filters were washed repeatedly with sodium phosphate buffer until no measurable amount of fluorescein remained on the coil surfaces. The deposition fraction was calculated as the mass deposited on the coil divided by the product of the average upstream concentration and the total volume of air passing through the coil. The experiments and analysis are described in greater detail in Siegel (2002).

3. Results and discussion

3.1. Modeling

Over the range of parameter values studied, deposition fraction was found to be a strong function of particle diameter and a weaker function of air velocity and fin spacing. Plots of deposition fraction appear in Figs. 3 and 4. For all except the smallest particles considered, deposition increases with increasing particle size. Deposition fractions for all velocities and fin spacings are $<2\%$ for submicron particles. Brownian diffusion is the dominant deposition mechanism that affects the smallest particles and the residence time in the coil is too short for Brownian diffusion to cause significant deposition. Deposition for $1\text{--}10\ \mu\text{m}$ particles is caused by impaction on fin edges. The kinks observed in Figs. 3 and 4 at $3\text{--}6\ \mu\text{m}$ aerodynamic diameter result from complete deposition on the fin from the volume of aligned, approaching air (i.e. the parenthetical term in Eq. (1) equals one, so P_{fin} is equal to $cf I_{\text{fin}} w^{-1}$). Deposition of particles $>10\ \mu\text{m}$ in diameter is caused by gravitational settling, impaction on tubes, and air turbulence. At a given fin spacing, impaction on refrigerant tubes is the dominant deposition mechanism for these larger particles at the higher velocities, and

Fig. 3. Modeled fractional deposition as a function of particle diameter for different air velocities and for fin spacing = $4.7\ \text{fin cm}^{-1}$.Fig. 4. Modeled fractional deposition as a function of particle diameter for different fin spacings and for $U = 2\ \text{m s}^{-1}$.

settling on fin corrugations is the predominant deposition mechanism for lower air velocities. Air turbulence impaction only contributes to the deposition of very large particles ($>50\ \mu\text{m}$).

Deposition increases with increased velocity for the inertial deposition mechanisms (impaction on fin edges and tubes and air turbulence impaction). Deposition decreases with increasing velocity for Brownian diffusion (this effect is hard to see in Figs. 3 and 4 because so little deposition occurs by this mechanism), and also for gravitational settling. Increased gravitational settling can be seen by the increased deposition for $8\text{--}12\ \mu\text{m}$ particles for $1\ \text{m s}^{-1}$ as compared with the higher velocities in Fig. 3. These increases are caused by the increased residence time for particles in the system at slower velocities. Deposition fraction increases with increased fin density for all particle sizes.

The estimated upper and lower bounds on deposition fraction are shown in Fig. 5 for an air velocity of $2\ \text{m s}^{-1}$ and a fin spacing of $4.7\ \text{fin cm}^{-1}$. The upper and lower

bounds on deposition fraction closely match the shape of the best estimate curve. Other velocities and fin spacings have similar shapes and magnitudes as those depicted in Fig. 5. The uncertainty is relatively small for particles <10 μm in diameter and is related to the uncertainty associated with fin edge impaction deposition. The larger uncertainty for larger particles is predominantly associated with gravitational settling, particularly for the upper bound on deposition fraction, with a contribution from refrigerant tube impaction. Air turbulence impaction contributes to overall uncertainty only for particles 80 μm and larger.

3.2. Measured deposition fraction

Deposition fraction is plotted as a function of aerodynamic diameter for three airspeeds in Figs. 6–8. Particle deposition increases on heat exchangers with increasing diameter. There is also evidence, for most particle sizes, of increasing deposition with increasing

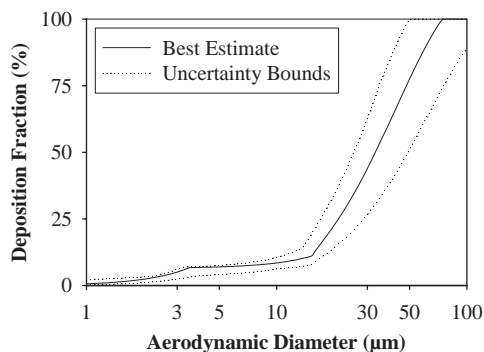


Fig. 5. Overall uncertainty bounds on modeled fractional particle deposition for $U = 2 \text{ m s}^{-1}$ and fin spacing = 4.7 fin cm^{-1} .

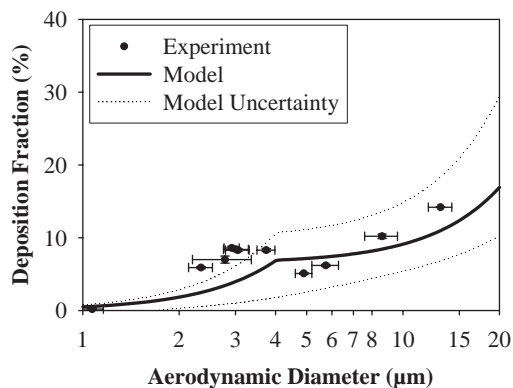


Fig. 6. Modeled and measured deposition fraction versus particle diameter for $U = 1.5 \text{ m s}^{-1}$ and fin spacing = 4.7 fin cm^{-1} .

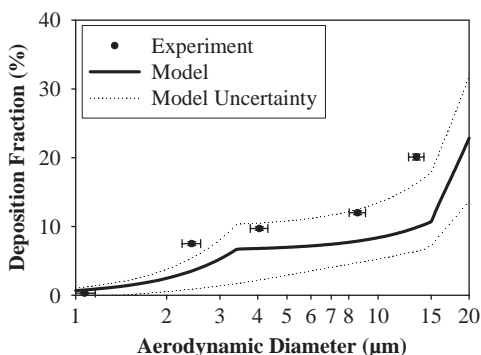


Fig. 7. Modeled and measured deposition fraction versus particle diameter for $U = 2.2 \text{ m s}^{-1}$ and fin spacing = 4.7 fin cm^{-1} .

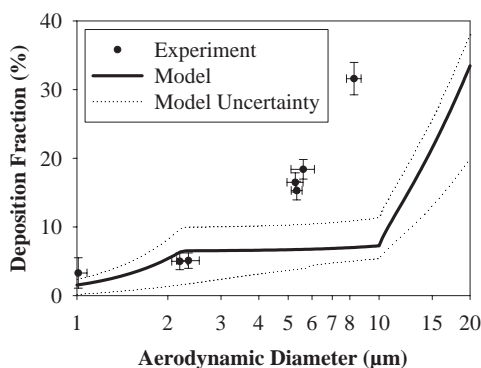


Fig. 8. Modeled and measured deposition fraction versus particle diameter for $U = 5.2 \text{ m s}^{-1}$ and fin spacing = 4.7 fin cm^{-1} .

airspeed. The horizontal error bars, indicating the polydispersity of the particles used in the experiment, show one standard deviation in particle aerodynamic diameter. The vertical error bars, which are difficult to see for some smaller particles and lower velocities, reflect the results of a propagation-of-error analysis. The uncertainty of the deposition fraction for 5.2 m s^{-1} (Fig. 8) is larger than for the other two velocities, apparently because of the resuspension of deposited particles from previous experiments. Two sets of experiments were repeated three times for 3 μm particles at 1.5 m s^{-1} and 5.5 μm particles at 5.2 m s^{-1} to test the validity of the experimental uncertainty analysis. These repeated experiments show an overlap of the vertical error bars from each repeated experiment and suggest good agreement between the predicted and measured experimental uncertainty. For comparison, the results of the simulations described above are also shown on each plot.

3.3. Model-measurement agreement

There is good qualitative agreement between the shape of the model and the measured results. There is reasonable agreement, on average, between magnitude of the modeled and measured deposition fractions. The model-measurement agreement diminishes with increasing air velocity, and at 2.2 and 5.2 m s⁻¹ air velocities, some experimental results can fall outside of the model uncertainty bounds. The simulations, with a few exceptions, tend to underpredict the measured deposition fractions. In the measured data, the deposition fractions increase with increasing particle diameter at smaller diameters than the model predicts. We hypothesize that this discrepancy is due to macroscale surface roughness elements and fin discontinuities that occur in HVAC heat exchangers, including the heat exchanger we tested. The increase in modeled-measured discrepancy at the highest velocity is hypothesized to be caused by additional turbulence. Detailed studies of turbulence within an HVAC heat exchanger would assist in testing this hypothesis.

4. Conclusions

We have carried out a mechanistic analysis of particle behavior to predict deposition on heat-exchanger surfaces, incorporating typical velocity and geometric parameters from HVAC heat exchangers. Fractional deposition ranges from <2% for small particles (<1 μm) to 50–100% for large particles (>50 μm). Greater air velocity leads to increased deposition by impaction on fin edges, tubes, and by air turbulence. Lower velocities cause increased deposition by Brownian diffusion and gravitational settling. Greater fin pitch leads to increased deposition by all mechanisms except for impaction on tubes which is essentially unaffected by fin pitch. Measurements reasonably confirm the modeled results, especially for low velocities and smaller particle sizes.

The results presented in the paper provide an important step towards a complete model of HVAC heat-exchanger fouling. These results and methods, in combination with information on indoor particle concentrations and airflow rates, can be used to estimate the mass deposited on a heat exchanger. The deposited mass would cause increased pressure drop and, if severe enough, performance problems. Further progress in understanding heat-exchanger fouling will require experiments that establish a relationship between deposited mass and increased pressure drop as well as a relationship between increased pressure drop and performance degradation. The results presented here can also be used to predict the deposition of bioaerosols on heat-exchanger surfaces. Future research should

examine particle deposition on cooled and condensing surfaces, contributing to a more complete understanding of particle deposition in real HVAC systems. Accurate predictions of deposition fraction and the effect of deposited particles will allow better evaluation of the cost and impacts of filtration and heat-exchanger cleaning.

Acknowledgements

This study was sponsored by the California Institute for Energy Efficiency (CIEE), a research unit of the University of California (Award No. BG-90-73). Publication of research results does not imply CIEE endorsement of or agreement with these findings, nor that of any CIEE sponsor. Support was also provided by the Office of Research and Development, Office of Nonproliferation and National Security, and the Office of Building Technology, State, and Community Programs, Office of Building Research and Standards, US Department of Energy under contract DE-AC03-76SF00098.

References

- Anand, N.K., McFarland, A.R., Kihm, K.D., Wong, F.S., 1992. Optimization of aerosol penetration through transport lines. *Aerosol Science and Technology* 16, 105–112.
- Bott, T.R., 1988. Gas side fouling. In: Melo, L.F., Bott, T.R., Bernardo, C.A. (Eds.), *Fouling Science and Technology*. Kluwer Academic Publishers, Dordrecht, pp. 191–206.
- Bott, T.R., 2001. To foul or not to foul, that is the question. *Chemical Engineering Progress* 97 (11), 30–37.
- Bott, T.R., Bemrose, C.R., 1983. Particulate fouling on the gas-side of finned tube heat-exchangers. *Journal of Heat Transfer* 105, 178–183.
- Bouris, D., Bergeles, G., 1996. Particle–surface interactions in heat exchanger fouling. *Journal of Fluids Engineering* 118, 574–581.
- Braun, M.J., Kudriavtsev, V.V., 1995. Fluid-flow structures in staggered banks of cylinders located in a channel. *Journal of Fluids Engineering* 117, 36–44.
- Caporaloni, M., Tampieri, F., Trombetti, F., Vittori, O., 1975. Transfer of particles in nonisotropic air turbulence. *Journal of the Atmospheric Sciences* 32, 565–568.
- Chen, Y.K., Yu, C.P., 1993. Particle deposition from duct flows by combined mechanisms. *Aerosol Science and Technology* 19, 389–395.
- DeMarcus, W., Thomas, J.W., 1952. Theory of a diffusion battery. Oak Ridge National Laboratory, ORNL-1413.
- Epstein, N., 1988. Particulate fouling of heat transfer surfaces: mechanisms and models. In: Melo, L.F., Bott, T.R., Bernardo, C.A. (Eds.), *Fouling Science and Technology*. Kluwer Academic Publishers, Dordrecht, pp. 143–164.
- Fuchs, N.A., 1964. *The Mechanics of Aerosols*. Pergamon Press, Oxford, New York.

- Hinds, W.C., 1999. *Aerosol Technology: Properties, Behavior, and Measurement of Airborne Particles*, 2nd Edition. Wiley, New York.
- Hinze, J.O., 1959. *Turbulence*. McGraw Hill, New York.
- Hugenholtz, P., Fuerst, J.A., 1992. Heterotrophic bacteria in an air-handling system. *Applied and Environmental Microbiology* 58, 3914–3920.
- Ilias, S., Douglas, P.L., 1989. Inertial impaction of aerosol-particles on cylinders at intermediate and high Reynolds-numbers. *Chemical Engineering Science* 44, 81–99.
- Israel, R., Rosner, D.E., 1983. Use of a generalized Stokes number to determine the aerodynamic capture efficiency of non-Stokesian particles from a compressible gas-flow. *Aerosol Science and Technology* 2, 45–51.
- Lipatov, G.N., Grinshpun, S.A., Semenyuk, T.I., 1988. Deposition of aerosol-particles in horizontal and inclined sampling tubes (experimental-data). *Journal of Aerosol Science* 19, 1059–1060.
- Melo, L.F., Bott, T.R., Bernardo, C.A., 1988. *Fouling Science and Technology*. Kluwer Academic Publishers, Dordrecht.
- Morey, P.R., 1988. Microorganisms in buildings and HVAC systems: a summary of 21 environmental studies. In: *ASHRAE IAQ '88*. American Society for Heating Refrigeration and Air-Conditioning Engineers, Atlanta, pp. 10–24.
- Moser, R.D., Kim, J., Mansour, N.N., 1999. Direct numerical simulation of turbulent channel flow up to $Re_\tau = 590$. *Physics of Fluids* 11, 943–945.
- Mukherjee, R., 1996. Conquer heat exchanger fouling. *Hydrocarbon Processing* 75 (1), 121–127.
- Muyschondt, A., Nutter, D., Gordon, M., 1998. Investigation of a fin-and-tube surface as a contaminant sink. In: *ASHRAE IAQ '98*. American Society for Heating Refrigeration and Air-Conditioning Engineers, Atlanta, pp. 207–211.
- Petermeier, H., Benning, R., Delgado, A., Kulozik, U., Hinrichs, J., Becker, T., 2002. Hybrid model of the fouling process in tubular heat exchangers for the dairy industry. *Journal of Food Engineering* 55 (1), 9–17.
- Pich, J., 1972. Theory of gravitational deposition of particles from laminar flows in channels. *Aerosol Science* 3, 351–361.
- Proctor, J., 1998. Monitored in-situ performance of residential air-conditioning systems. *ASHRAE Transactions* 104 (1B), 1833–1840.
- Rampall, I., Singh, K.P., Soler, A.I., Scott, B.H., 1997. Application of transient analysis methodology to quantify thermal performance of heat exchangers. *Heat Transfer Engineering* 18 (4), 22–34.
- Siegel, J., 2002. *Particle Deposition on HVAC Heat Exchangers*. Ph.D. Dissertation, Department of Mechanical Engineering, University of California, Berkeley.
- Somerscales, E.F.C., Knudsen, J.G., 1981. *Fouling of Heat Transfer Equipment*. Hemisphere Pub. Corp., Washington.
- Tabourek, J., Aoki, T., Ritter, R.B., Palen, J.W., Knudsen, J.G., 1972. Fouling: the major unresolved problem in heat transfer. *Chemical Engineering Progress* 68 (2), 59–67.
- Wang, H.C., 1986. Theoretical adhesion efficiency for particles impacting a cylinder at high Reynolds-number. *Journal of Aerosol Science* 17, 827–837.